Kovove Mater. 59 2021 59–68
DOI: 10.4149/km_2021_1_59

Determination of the thermal properties of Al-Zn-Mg alloy

E. Çadırlı[1]*, E. Üstün[2], U. Büyük[3], H. Kaya[3]

[1]*Niğde Ömer Halisdemir University, Faculty of Arts and Sciences, Department of Physics, Niğde, Turkey*
[2]*Niğde Ömer Halisdemir University, Institute of Science and Technology, Niğde, Turkey*
[3]*Erciyes University, Faculty of Education, Department of Science Education, Kayseri, Turkey*

Received 3 August 2020, received in revised form 7 September 2020, accepted 10 October 2020

Abstract

In this work, the thermal conductivity, enthalpy of fusion, specific heat capacity, and thermal diffusivity of the Al-5.5Zn-2.5Mg (wt.%) ternary alloy have been investigated. Thermal conductivity of as-cast Al-5.5Zn-2.5Mg alloy was measured using comparison cut bar method in the temperature range of 323–723 K. With the increase of temperature, thermal conductivity decreased gradually in as-cast Al-5.5Zn-2.5Mg alloy. The thermal temperature coefficient was calculated from the respective graph. The enthalpy of fusion and the specific heat capacity during the transformation were also determined. Thermal diffusivity changes were calculated as a function of temperature through the obtained thermal data. It was observed that thermal diffusivity values decreased with increasing temperature.

K e y w o r d s: 7XXX alloys, thermal conductivity, thermal diffusivity, specific heat capacity, enthalpy of fusion

1. Introduction

7075 Al alloy (7XXX series), with its good machinability and weldability, is widely used in welded engineering structural components, military applications, cryogenic pressure vessels, components of spacecraft liquid-propellant engines, and bridge beams for road systems and in aerospace applications. In space applications, this material may be subjected to extreme environmental conditions, including both low and high temperatures, high pressures and highly corrosive and reactive fluids [1–3]. Thermal parameters such as thermal conductivity, thermal diffusivity and specific heat have a strong influence on the cold forming, hot forming and weld penetration. Selecting appropriate process parameters is difficult, which necessitates the need to build a relationship between the processing parameters and the quality of the weld joint [4]. In the experimental determination of the thermal conductivity (K) of solids, several different methods of measurement are required for different ranges of temperature and various classes of materials having different ranges of K values.

Thermal conductivity measurement methods are typically classified into two categories: steady-state and transient. Steady-state measurement employs a constant temperature gradient in the sample, whereas transient measurement relies on a pulse or continuous heating with subsequent dynamic temperature monitoring. Though typically characterized by quick measurement times and simple setups, transient measurement methods such as hot wire [5], hot plate or hot disk [6], thermal probe [7–9], laser flash [10], and line source [11] or the recently developed photo-acoustic [12] and photo-thermal [13] methods were excluded as potential measurement options for this work due to the fuel compact's geometry and composition as well as the non-destructive requirement. Though the main principle on which steady-state thermal conductivity measurement methods are based is quite simple (Fourier's law), such measurement methods often require a complex, carefully designed and operated experimental setup. Steady-state and transient methods may be further categorized as either absolute or comparative based on whether the heat flux in the sample is measured directly (e.g., power input to a heater) or is calculated based on a comparison with the heat flux in an adjacent reference sample with

*Corresponding author: e-mail address: ecadirli@gmail.com

known properties. Standard steady-state methods include the guarded hot plate [14], the radial heat flow [15], the axial heat flow [16–18], and the direct heating [19] methods. For this work, the comparative-guarded--axial heat flow or comparative cut bar method was selected for the studied alloy. This method has been widely employed in scientific studies and industry. However, reports of detailed uncertainty analysis are limited. The precision error associated with the heat flux equation used to calculate thermal conductivity in this method has been discussed [20, 21] whereas systematic error analysis associated with geometries and reference and sample thermal conductivity mismatch was found only [22].

Thermal transport in metals is complex due to the coexistence of electron and phonon conduction and the strong interaction between them. The total thermal conductivity (K_{tot}) has two components: The electronic thermal conductivity (K_{e}) and the lattice (or phonon) thermal conductivity (K_{L}). The total thermal conductivity is the sum of these two components:

$$K_{\mathrm{tot}} = K_{\mathrm{e}} + K_{\mathrm{L}}. \tag{1}$$

The contribution of electrons is more significant than that of phonon at all temperatures in pure metals.

There are many studies on the measurement of thermal conductivity of different Al-based alloys under various experimental conditions (heat treatment, extrusion, hot forging, etc.). However, the research on the commercially crucial Al-5.5Zn-2.5Mg alloy is scarce. There are very few studies in the literature that measure the change in thermal conductivity depending on temperature for a similar alloy [23–25].

Li and Yu [23] studied the thermal conductivity of the Al-6.1Zn-2.3Mg-1.9Cu (wt.%) alloys at various heat treatment conditions (solution treated at 748 K and aged at 445 K for 4 h). The results show that the thermal conductivity decreased gradually with the increase of temperature in the temperature range of 450–725 K. Hamilton et al. [24] investigated the behavior of thermal conductivity and specific heat capacity for AA7050 (Al-5.6Zn-2.5Mg-1.6Cu (wt.%)) alloy produced by chill casting method depending on the increasing temperature. They observed that the thermal conductivity decreased, and the specific heat capacity increased in the temperature range of 550–700 K. Murthy et al. [25] reported the thermal conductivity values for AA7075 (Al-3.25Zn-1.9Mg-1.8Cu (wt.%)) and hybrid composites at different TiO_2 weight fraction and different temperatures. They found that the thermal conductivity decreased for both the AA7075 alloy and the composite alloys depending on the increasing temperature. Also, they have observed that the thermal conductivity of hybrid composites was lower than that of unreinforced AA7075 alloy.

In this study, Al-5.5Zn-2.5Mg alloy is preferred because of its good machinability and weldability. The difference in our research from other studies is that thermal properties have been investigated in a wide temperature range ($\sim$ 323–723 K) without any heat treatment or mechanical process. Thus, the purpose of this work was to determine the thermal conductivities (K), thermal diffusivity, and specific heat of studied alloy depending on temperature. Experimental processes were carried out in three steps. In the first step, the variation of thermal conductivity of Al-5.5Zn-2.5Mg alloy was measured in the range of temperature ($\sim$ 323–723 K) by using comparative cut bar method. In the second step, the enthalpy of fusion (ΔH) and the specific heat capacity (C_{p}) during the transformation were determined with Differential Scanning Calorimetry (DSC). In the third step, thermal diffusivity (α) changes were calculated as a function of temperature based on the obtained thermal data for the studied alloy.

2. Experimental procedure

2.1. Sample preparation

For Al-5.5Zn-2.5Mg ternary alloy, the quantities of the metals were determined by making stoichiometric calculations, and it was paid attention that the metals used in the preparation of this ternary alloy were significantly higher than of 99.9 % purity (alloys attributed in this study were given by weight per cent unless otherwise stated). When an alloy material with insufficient purity is prepared, impurities accumulate on the interface and negatively affect the structure shapes formed on the interface during the experimental process. First, Al was placed in a graphite mold and melted in a vacuum furnace. After the Al melted utterly, the required amount of Zn (5.5 wt.%) was placed under the surface of the liquid Al. Three stirrings of the liquid Al-Zn alloy were carried out at five-minute intervals and then required amount of Mg (2.5 wt.%) packed with pure thin Al foil was placed in a graphite cage with many perforations; it was then put under the surface of the liquid Al-Zn alloy to avoid Mg burning on the surface of the melt. Homogeneously prepared melt alloy, without any air bubbles, was poured into the previously prepared (4 mm ID, 6.35 mm OD and 250 mm in length) graphite crucibles placed inside the casting furnace (Fig. 1).

2.2. Measurement of the thermal conductivity K

The measurements were carried out on as-cast samples. So, no heat treatment had been applied. In the comparative cut bar method, a test sample of un-

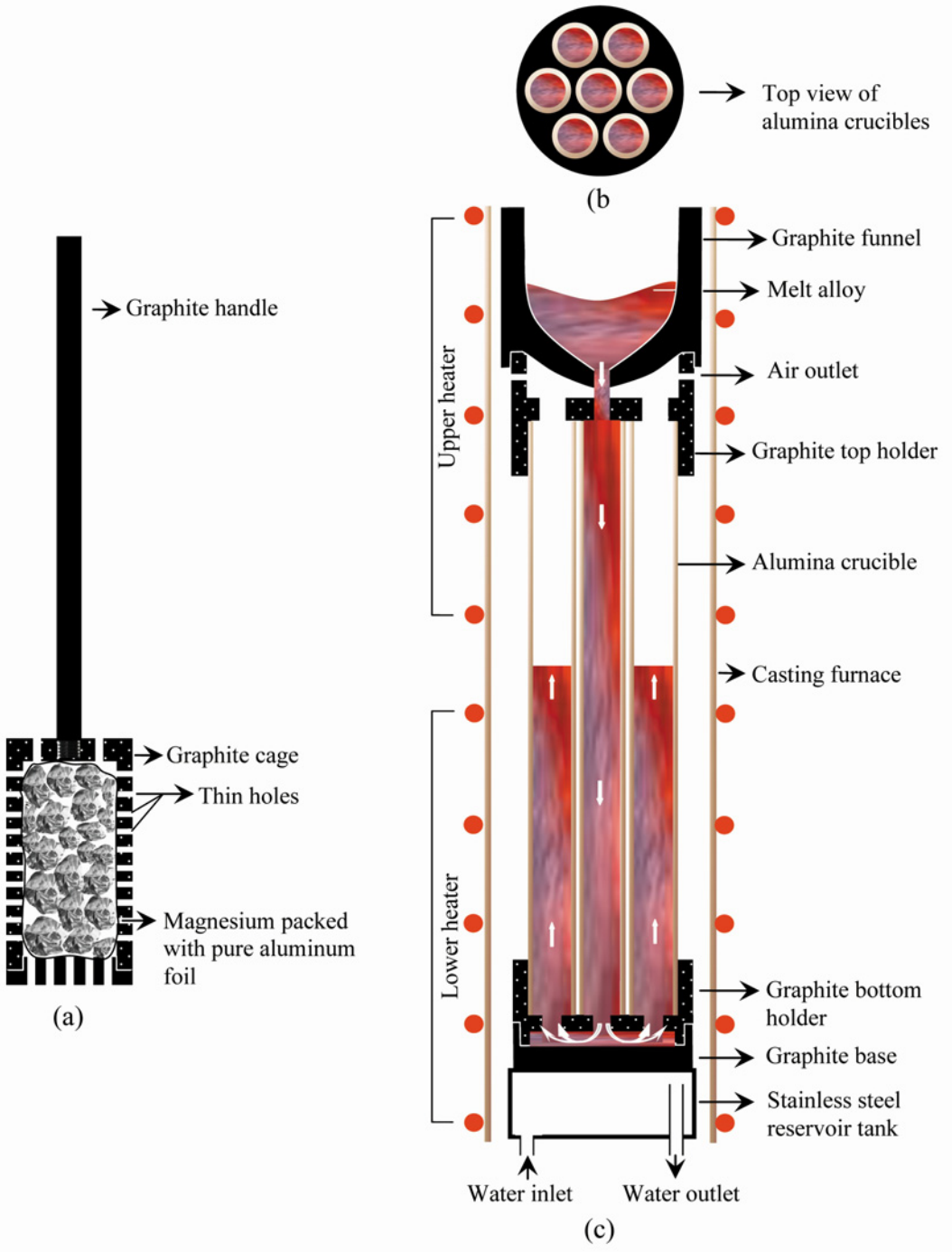

Fig. 1. (a) Graphite cage, (b) top view of alumina crucibles, and (c) crucibles in the casting furnace.

known thermal conductivity is sandwiched between two reference material (pure Al) with known thermal conductivity using thermal grease and a pliable metal foil to eliminate interfacial thermal contact resistance between the materials. Before the sandwiching process, each of these materials (the test and reference samples) was cut into 12 mm length and drilled 0.7 mm in diameter from the center for a thermocouple placement. Then, the surfaces of each sample were polished to minimize contact resistance at the interfaces. Thermocouples placed along the length of the three material pieces yield information on the rate of heat flow through the two reference-material sections of known conductivity. The heat-flow rate can then be used to determine the thermal conductivity of the unknown sample using the one-dimensional Fourier conduction equation, Eq. (2):

$$Q = -KA\frac{\mathrm{d}T}{\mathrm{d}x}, \tag{2}$$

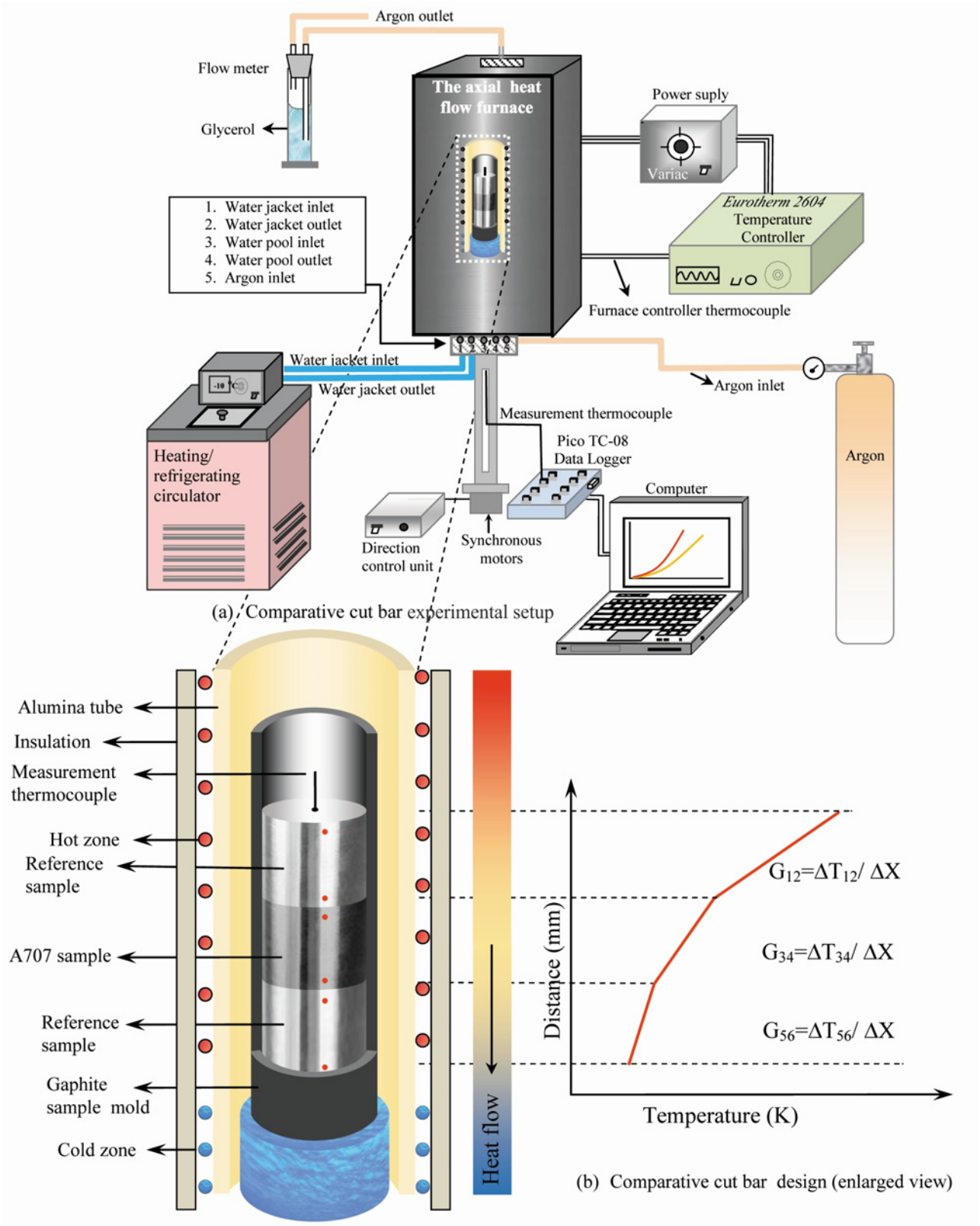

Fig. 2. Schematic illustration of the experimental setup: (a) comparative cut bar experimental setup and (b) comparative cut bar design (enlarged view).

where Q is the rate of heat flow, K is the thermal conductivity, A is the cross-sectional area through which the heat flows, and $\mathrm{d}T/\mathrm{d}x$ is the temperature gradient. Experimentally, $\mathrm{d}T$ is approximated by ΔT, the

finite temperature difference, and $\mathrm{d}x$ is approximated by Δx, the distance over which the temperature difference is measured.

Figure 2 shows a schematic diagram of the comparative-longitudinal-heat flow method. In this method, a test sample (as-cast condition) of unknown thermal conductivity (K_s) is sandwiched between two reference samples (pure Al) of known thermal conductivity (K_r) in axial heat flow furnace. A temperature gradient, $\Delta T/\Delta X$ is set up through the samples such that it may be measured in each of the three samples. The heat flux through the unknown sample can be calculated from the Eq. (3):

$$\frac{Q}{A} = -K_\mathrm{s}\frac{\Delta T_{34}}{\Delta X_{34}} = \frac{K_\mathrm{r}}{2}\left(\frac{\Delta T_{12}}{\Delta X_{12}} + \frac{\Delta T_{56}}{\Delta X_{56}}\right). \qquad (3)$$

As can be seen in Fig. 2, the axial heat flow furnace has three main parts. There are hot and cold regions in the furnace to create a vertical temperature gradient in the test sample and reference sample. The driving system mounted under the furnace ensures that the samples come in the appropriate region. To get an axial heat flow, cylindrical samples are heated from the top and cooled from the bottom with the water cooling system. Lateral heat flow can be reduced with suitable insulation. The experimental system is also capable of operating under an inert gas atmosphere. A vacuum is not recommended for this type of measurement [16] as it can increase the thermal contact resistance. The lateral heat loss is more critical than the reduced contact resistance in this case because of the large ratio of lateral surface area to sample-column (radial) interfacial area. For this reason, lower conductivity argon has been selected to provide the inert environment.

The furnace was heated in steps of 50 K from the room temperature up to approximately 800 K. The temperature of the furnace was controlled to an accuracy of ± 0.1 K with a *Eurotherm 2604* type controller. The samples (test and reference) were kept at steady state condition for at least two hours for a setting temperature. At the steady-state condition, the temperatures of the axial position of the samples (red points) were measured with a mineral insulated metal sheathed, and 0.5 mm in diameter K-type thermocouples were moved through the center of cylindrical samples (Fig. 2b). All measurement thermocouples were connected to a *Pico TC-08* data-logger unit. A computer was used to record all the data. The error in the thermal conductivity measurements was calculated to be about 5 %.

The dependence of K of the solid phase on temperature can be expressed as

$$K = K_0[1 + \alpha_\mathrm{TTC}(T - T_0)] \qquad (4a)$$

and the thermal temperature coefficient, $\alpha_\mathrm{TTC,}$ is expressed as [10]:

$$\alpha_\mathrm{TTC} = \frac{K - K_0}{K_0(T - T_0)} = \frac{1}{K_0}\frac{\Delta K}{\Delta T}, \qquad (4b)$$

where K is the thermal conductivity at the temperature T, K_0 is the thermal conductivity at the room temperature (T_0).

2.3. Determination of ΔH, C_p and thermal diffusivity

Differential scanning calorimetry (DSC) is carried out together with thermogravimetric (TG) analysis of the sample, using a *Netzsch STA 449 C Jupiter balance*. The DSC curve shows the amount of heat required to increase the temperature of a sample; the specific heat capacity, C_p, is determined by

$$mC_\mathrm{p}\frac{\mathrm{d}T}{\mathrm{d}t} = \frac{\mathrm{d}Q}{\mathrm{d}t}, \qquad (5)$$

where m is the mass of the sample, $\mathrm{d}T/\mathrm{d}t$ is heating rate, and $\mathrm{d}Q/\mathrm{d}t$ is heat flow. A reference sample with a well-defined specific heat capacity, sapphire in this study, was measured together with the sample. The heat flux and temperature difference between the sample and the reference throughout the heating and/or cooling were measured, and the specific heat capacity of the sample was determined by using Eq. (5). Measurements of thermal properties were carried out during heating and subsequent cooling regimes at a rate of 5 K min^{-1} under argon flow (50 mL min^{-1}). The accuracy of determination of the temperature and enthalpy of reactions were ± 0.2 K and ± 5 %, respectively.

Another important variable in defining the thermal properties of a material is thermal diffusivity. This is a measurement of the rate at which a material can adapt to a thermal disturbance travelling through it. Whereas thermal conductivity measures the rate at which thermal energy travels through a body, thermal diffusivity deals specifically with the associated rise in temperature measured in m^2 s^{-1}. After measuring the thermal conductivity using comparative cut bar method, the thermal conductivity was substituted into Eq. (6) to calculate the thermal diffusivity:

$$\alpha = \frac{K}{\rho C_\mathrm{p}}, \qquad (6)$$

where α is the thermal diffusivity, K is the thermal conductivity, ρ is the density, and C_p is the specific heat capacity. Densities at elevated temperatures were calculated using Eq. (7):

$$\rho(T) = \frac{\rho T_\mathrm{RT}}{(1 - \alpha_\mathrm{T}(T - T_\mathrm{RT}))^3}, \qquad (7)$$

Table 1. The chemical composition analysis with direct current plasma emission spectroscopy (DPES) of the studied alloy (Al-5.5Zn-2.5Mg)

Element	Zn	Mg	Cu	Fe	Cr	Mn	Si	Ti	Al
(wt.%)	5.72	2.48	0.12	0.10	0.16	0.18	0.11	0.06	Balance
Error (%)	0.03	0.02	0.03	0.007	0.009	0.006	0.02	0.003	0.3

where α_T is the thermal expansion coefficient and T_{RT} is the room temperature.

3. Results and discussion

3.1. Characterization of the phases and compositions

The verified compositions in Table 1 were obtained from the studied alloy system by the bulk chemical analysis performed with direct current plasma emission spectroscopy (DPES). DPES analysis was repeated three times for the cast samples, and the mean and error percentages were calculated. As seen in Table 1, the composition quantities of Al, Zn, Mg, and other impurities were found to be 91.07, 5.72, 2.48, and 0.73 %, respectively. These values are in agreement with the nominal compositions of the samples. XRD data for phase identification of Al-5.5Zn-2.5Mg alloy are shown in Fig. 3. In cast condition, alloy exhibited peaks for α-Al, $MgZn_2$ (η), and Al_2CuMg (S) phases. Peaks (black squares) at 38.4°, 44.4°, 64.9°, and 78° correspond to α-Al phase. Peaks (red triangles) at 39.7°, 40.6°, 41.8°, and 64.9° correspond to intermetallic hexagonal $MgZn_2$ (η) intermetallic phase. Peaks (blue circles) at 78° and 82.2° correspond to intermetallic orthorhombic Al_2CuMg (S) intermetallic phase. Peaks which fit many phases show the possibility to exist with only the XRD result. Therefore, analyzing together with other methods such as EDX or DPES is necessary to determine whether the phase really exists or not. The DPES analysis results in Table 1 confirm the XRD-detected phases in Fig. 3. Both DPES analysis (Table 1) and XRD pattern (Fig. 3) strongly indicate that only three phases (α-Al, $MgZn_2$, and Al_2CuMg) are present in the microstructure of the cast sample.

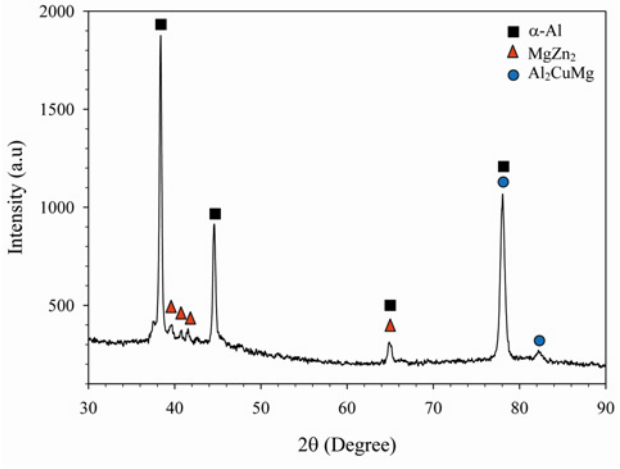

Fig. 3. X-ray diffraction (XRD) patterns obtained from the Al-5.5Zn-2.5Mg alloy.

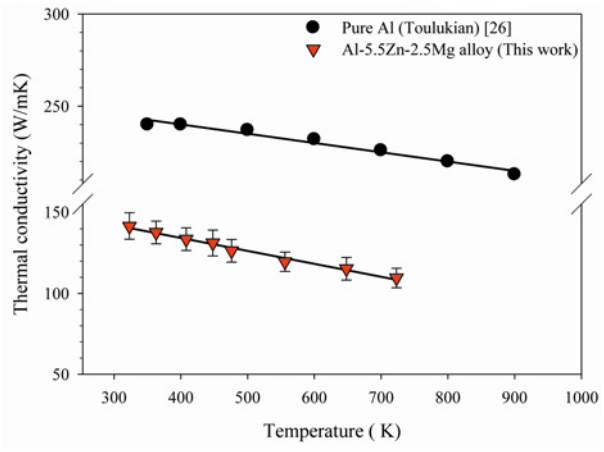

Fig. 4. The variation of thermal conductivities with temperature for Al-5.5Zn-2.5Mg alloy and pure Al.

3.2. Dependence of K on the temperature

Figure 4 illustrates the K values of the studied alloy and pure Al [26] with temperature. As can be seen from the graph, K values decrease with increasing temperature. As can be seen in Fig. 5, the K values of pure Al [26], pure Zn [26], pure Mg [27], studied alloy and some Al alloys [23–25, 28–31] decrease with increasing temperature, and the measured lines of K variations with temperature for the Al-5.5Zn-2.5Mg alloy are fairly below the line of K variation with temperature for pure Al [26], pure Mg [27], Al-1Mg alloy [28], Al-5Zn [29], Al-0.7Mg-0.4Si [30], Al-6.1Zn-2.3Mg-1.9Cu [23], and Al-5.6Zn-2.5Mg-1.6Cu [24]. Also, the K values obtained for the studied alloy (Table 2) were slightly higher than those obtained for pure Zn [26], 7075/AlN composite [31], and Al-3.25Zn-1.9Mg-1.8Cu alloy [25]. In the case of pure

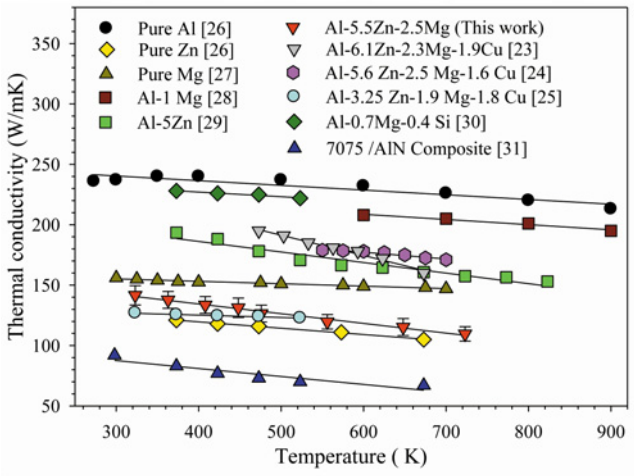

Fig. 5. The variation of thermal conductivities with temperature for the pure Al, pure Zn, pure Mg, Al-5.5Zn-2.5Mg alloy, and other Al-based alloys.

Al and pure Zn, there were relatively fewer impurities, such as solute atoms of Mg and Zn in α-Al matrix. So, the scattering of an electron by impurity was weak. With the increase of temperature, the vibration of lattice became more severe, which strongly impeded the movement of both electrons and phonons; thus, the electron-phonon and phonon-phonon scattering became dominant at higher temperature range, leading to lower thermal conductivity. According to Fig. 5, with increasing temperature, the values of K decreased from 240, 156, 141, and 121 $\mathrm{W\,m^{-1}\,K^{-1}}$ to 213, 147, 109, and 105 $\mathrm{W\,m^{-1}\,K^{-1}}$, for the pure Al [26], pure Mg [27], Al-5.5Zn-2.5Mg, and pure Zn [26], respectively. Some studies on this subject for binary (Al-Zn, Al-Mg), ternary (Al-Mg-Si), and quaternary (Al-Zn-Mg-Cu) alloys have been examined, and some main results are summarized below.

Erol et al. [29] examined the thermal conductivity of the radial heat flow applied to Al-5Zn alloy. They found that thermal conductivity decreased from 182 to 144 $\mathrm{W\,K^{-1}\,m^{-1}}$ with increasing the temperature from 373 to 823 K. The authors determined the α_{TTC} value for this alloy as $0.00043\,\mathrm{K^{-1}}$. Besides, they also found in their studies that the increased amount of Zn decreased the thermal conductivity.

Ho et al. [28] performed heat treatment for the alloy with Al-1Mg composition and then determined the thermal conductivities for the (Al) solid solution. They reported that thermal conductivity decreased from 208 to 195 $\mathrm{W\,K^{-1}\,m^{-1}}$ in the range of 600–900 K.

Smith [30] investigated thermal conductivity behavior of the 6063-T1 (Al-0.7Mg-0.4Si) and reported that thermal conductivity decreased from 228 to 222 $\mathrm{W\,K^{-1}\,m^{-1}}$ in the range of 373–523 K. However, the author stated that the increasing Mg concentration has negative effects on the thermal conductivity

Table 2. Measured K values of the studied alloy in the range of 323–723 K

Temperature T (K)	Thermal conductivity K ($\mathrm{W\,m^{-1}\,K^{-1}}$)
323	141.6 ± 8
363	137.8 ± 7
408	133.6 ± 7
448	131.3 ± 8
476	126.4 ± 7
556	119.6 ± 6
648	115.3 ± 7
723	109.6 ± 6

of the alloy studied. It was postulated that this behavior was directly attributable to the influence of each element on the concentration of magnesium dissolved within the aluminum grains.

In another study, Murthy et al. [25] investigated the thermal conductivity of 7075 alloy (Al-3.25Zn--1.9Mg-1.8Cu) produced by stir casting technique followed by hot forging. They reported that thermal conductivity decreased from 127 to 122 $\mathrm{W\,K^{-1}\,m^{-1}}$ in the range of 323–523 K. Also, by these authors, different amounts of TiO_2 reinforcements were added to 7075 alloy and the change of K values according to both temperature and TiO_2 reinforcements was investigated. They reported that the K values clearly decreased with increasing temperature and amount of TiO_2 reinforcements.

Although K values obtained by us in the broader temperature range (323–823 K) are lower than the K values obtained by Smith [30] and Ho et al. [28], it is higher than the values obtained by Murthy et al. [25] and Erol et al. [29]. As seen from the results, not only temperature and composition are sufficient on thermal conductivity, but also heat treatment, mechanical processing, and minor additions of elements are effective. Generally, the addition of the alloying elements to alloys leads to the decrease of the thermal conductivity of the alloys. It is generally believed that the addition of the alloying elements destroyed the periodic arrangement of matrix atoms and impeded the movement of electrons in the crystal lattice to reduce the average free path of electrons, thereby reducing the thermal conductivity of the alloys.

α_{TTC} values of pure metals and worked alloy were calculated from the K-T curves seen in Fig. 5. The α_{TTC} values for the pure Al, pure Zn, pure Mg, and Al-5.5Zn-2.5Mg alloy were calculated as -2.25×10^{-4}, -4.41×10^{-4}, -1.40×10^{-4}, and -5.65×10^{-4} $\mathrm{K^{-1}}$ in the range of temperature 323–823 K, respectively, as can be seen in Table 3.

3.3. The ΔH, C_p, and thermal diffusivity (α)

The thermal properties of the Al-5.5Zn-2.5Mg al-

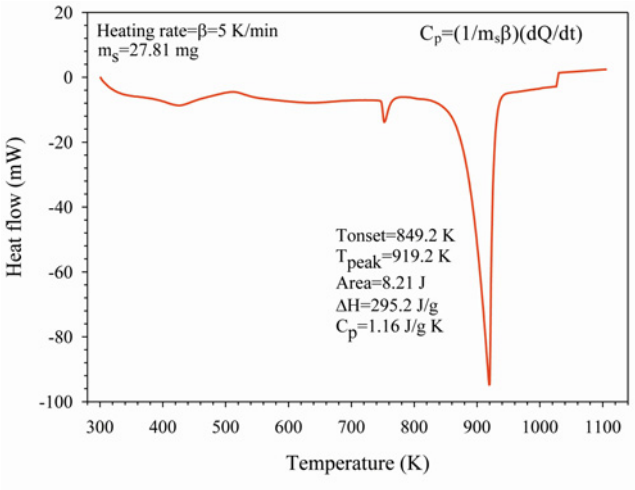

Fig. 6. The heat flow-temperature curve of Al-5.5Zn-2.5Mg alloy.

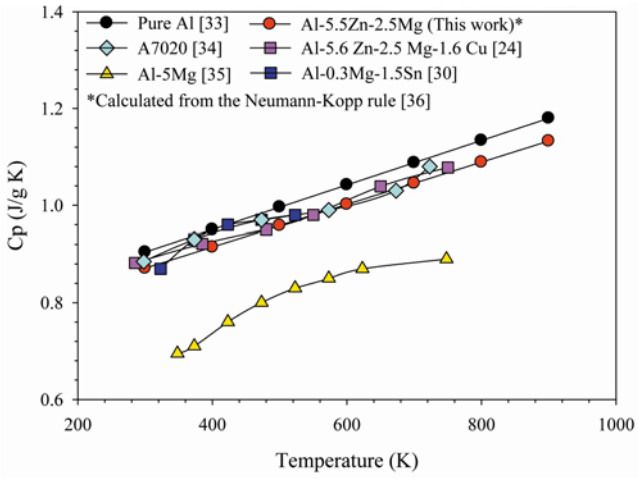

Fig. 7. The variation of specific heat capacity with temperature for the pure Al, Al-5.5Zn-2.5Mg alloy and other Al-based alloys.

Table 3. Calculated values of the α_{TTC} of the pure Al, pure Zn, pure Mg, and studied alloy in the range of 323–823 K

Material	$\alpha_{TTC} \times 10^{-4}$ (K^{-1})
Pure Al	–2.25 [26]
Pure Mg	–1.40 [27]
Pure Zn	–4.41 [32]
Al-5.5Zn-2.5Mg	–5.65 (This work)

loy such as ΔH, T_m, and C_p were investigated using a heating rate of 5 K min^{-1} in the range 300–1100 K with DSC analysis in a flow of purified argon. The

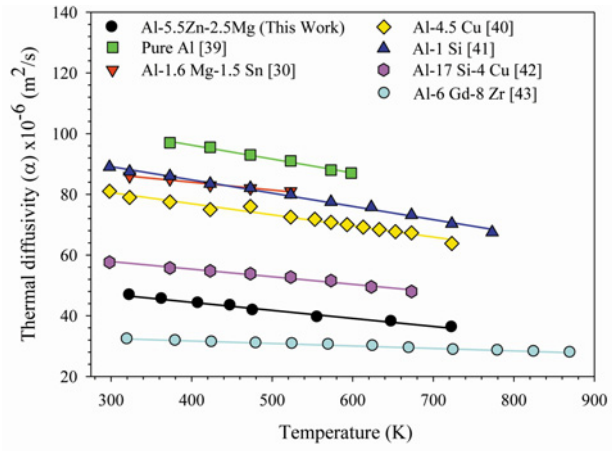

Fig. 8. Temperature dependence of the thermal diffusivity of the pure Al, Al-5.5Zn-2.5Mg alloy and other Al-based alloys.

variation of the heat flow with temperature is given in Fig. 6. A sharp peak occurred during melting. The melting temperature (T_{peak}) of the studied alloy was determined to be 919.2 K, the ΔH and C_P values were calculated as 295.2 J g^{-1} and 1.05 J g^{-1} K^{-1}, respectively. Figure 7 shows the temperature dependence of the calculated C_P for the pure Al [33], Al-5.5Zn-2.5Mg alloy and other Al-based alloys [24, 30, 34–36]. The empirical relationships [37, 38] used in the calculation of the C_P for solid and liquid phases of pure Al, Zn, and Mg are given in Table 4. According to Neumann-Kopp rule [36], the C_P of an alloy is equal to the sum of the products of the atomic fraction of the constituent elements, and their atomic C_P. $C_P - T$ change for the studied alloy was calculated numerically by Neumann-Kopp rule [36].

As can be seen in Table 4, C_P values for liquid phases of the pure Al, Zn, and Mg metals are generally constant while C_P in solid phases increased depending on the temperature. The thermal diffusivities were calculated by inserting the thermal conductivities, density, and specific heat data for studied alloy in Eq. (7). Density varies as a function of temperature as seen in Eq. (8). This situation was taken into consideration for the studied alloy. The values of thermal diffusivity decreased with increasing temperature. The temperature dependence of thermal diffusivity for the pure Al [39], studied alloy and some other Al-based alloys [30, 40–43] is shown in Fig. 8. With the increase of temperature from 323 to 723 K, the value of thermal diffusivity decreased from 46.8 $\times$ 10^{-6} to 36.2 $\times$ 10^{-6} m^2 s^{-1} for the Al-5.5Zn-2.5Mg alloy. The thermal diffusivity of the pure Al and other alloys decreased with increasing temperature. In the thermal diffusivity values for alloys being close to each other, dilution of alloys may play a dominant role.

Table 4. Specific heat capacities of the pure Al, Zn, and Mg metals

Material	C_P (liquid) (J g^{-1} K^{-1})	C_P (solid) (J g^{-1} K^{-1})
Pure Al	1.18 [37]	$4.94 + 2.96 \times 10^{-3}T$ [37]
Pure Zn	0.48 [38]	$5.35 + 2.4 \times 10^{-3}T$ [38]
Pure Mg	1.32 [37]	$5.33 + 2.45 \times 10^{-3}T - 0.10^{3} \times 10^{-5}T^{-2}$ [37]

4. Conclusions

The thermal conductivity, thermal diffusivity, ΔH, and C_P of the Al-5.5Zn-2.5Mg alloy were investigated. The results are summarized as follows:

1. The K of the Al-5.5Zn-2.5Mg alloy linearly decreases from 141.6 to 109.5 W m^{-1} K^{-1} with increasing temperatures from 323 to 723 K. The α_{TTC} value (–5.65 × 10^{-4} K^{-1}) for the studied alloy was determined from the graphs of K variation with temperature.

2. The measured melting temperature of the studied alloy was 919.2 K, and ΔH and C_P were calculated as 295.2 J g^{-1} and 1.05 J g^{-1} K^{-1} (in solid-liquid transition), respectively.

3. While the C_P values of the studied alloys increase with increasing temperature, the thermal diffusivity values decrease. The thermal diffusivity (calculated) decreased from 46.8 × 10^{-6} to 36.2 × 10^{-6} m^2 s^{-1} in the temperature range from 323 to 723 K, respectively.

Acknowledgements

This project was supported by Niğde Ömer Halisdemir University Scientific Research Project Unit Contract No: FEB 2016/08. The authors are grateful to Niğde Ömer Halisdemir University Scientific Research Project Unit for their financial support.

References

[1] R. E. Smallman, A. H. W. Ngan, Modern Physical Metallurgy, 8th. ed., Butterworth-Heinemann, New York, 2014.

[2] S. Kumar, T. K. G. Namboodhiri, Precipitation hardening and hydrogen embrittlement of aluminum alloy AA7020, Bull. Mat. Sci. 34 (2011) 311–321. doi:10.1007/s12034-011-0066-8

[3] G. S. Rao, V. V. S. Rao, S. R. K. Rao, Microstructure and mechanical properties of welded joints of aluminum alloy AA7020-T6 obtained by friction stir welding, Met. Sci. Heat Treat. 59 (2017) 139–144. doi:10.1007/s11041-017-0117-x

[4] L. Cao, Y. Yang, P. Jiang, Q. Zhou, G. Mi, Z. Gao, Y. Rong, C. Wang, Optimization of process parameters of AlSi 316L laser welding influenced by external magnetic field combining RBFNN and GA, Results Phys. 7 (2017) 1329–1338. doi:10.1016/j.rinp.2017.03.029

[5] M. J. Assael, M. Dix, K. Gialou, L. Vozar, W. A. Wakeham, Application of the transient hot-wire technique to the measurement of the thermal conductivity of solids, Int. J. Thermophys. 23 (2002) 615–633. doi:10.1023/A:1015494802462

[6] H. Wang, R. B. Dinwiddie, M. Gustavsson, S. E. Gustafsson, Infrared imaging during hot disk thermal conductivity measurements, Thermal Conductivity, Volume 28. In: R. B. Dinwiddie, M. A. White, D. L. McElroy (Eds.), Thermal Expansion, Thermal Conductivity Book Series, DEStech, Lancaster, 2016, pp. 199–207. ISBN 978-1-932078-59-6

[7] K. Manohar, D. Yarbrough, J. Booth, Measurement of apparent thermal conductivity by the thermal probe method, J. Test. Eval. 28 (2000) 345–351. doi:10.1520/JTE12123J

[8] P. de Wilde, R. Griffiths, S. Goodhew, Validation of data analysis routines for a thermal probe apparatus using numerical data sets, Build. Simul. 1 (2008) 36–45. doi:10.1007/s12273-008-8105-0

[9] P. de Wilde, R. Griffiths, S. Goodhew, Evolution and validation of a thermal probe model, J. Build. Perform. Simul. 2 (2009) 85–94. doi:10.1080/19401490802590693

[10] H. Mehling, G. Hautzinger, O. Nilsson, J. Fricke, R. Hofmann, O. Hahn, Thermal diffusivity of semitransparent materials determined by the laser-flash method applying a new analytical model, Int. J. Thermophys. 19 (1998) 941–949. doi:10.1023/A:1022611527321

[11] C. Le Niliot, F. Rigollet, D. Petit, An experimental identification of line heat sources in a diffusive system using the boundary element method, Int. J. Heat Mass Trans. 43 (2000) 2205–2220. doi:10.1016/S0017-9310(99)00285-9

[12] X. Wang, H. Hu, X. Xu, Photo-acoustic measurement of thermal conductivity of thin films and bulk materials, J. Heat Trans. 123 (2001) 138–144. doi:10.1115/1.1337652

[13] N. Taketoshi, T. Baba, A. Ono, Development of a thermal diffusivity measurement system for metal thin films using a picosecond thermoreflectance technique, Meas. Sci. Technol. 12 (2001) 2064–2073. doi:10.1088/0957-0233/12/12/306

[14] J. Xamán, L. Lira, J. Arce, Analysis of the temperature distribution in a guarded hot plate apparatus for measuring thermal conductivity, Appl. Therm. Eng. 29 (2009) 617–623. doi:10.1016/j.applthermaleng.2008.03.033

[15] M. Gündüz, J. D. Hunt, The measurement of solid-liquid surface energies in the Al-Cu, Al-Si, and Pb-Sn systems, Acta Metall. 33 (1985)1651–1672. doi:10.1016/0001-6160(85)90161-0

[16] J. M. Corsan, Axial Heat Flow Methods of Thermal Conductivity Measurement for Good Conducting Materials. In: K. D. Maglić, A. Cezairliyan, V.

E. Peletsky (Eds.), Compendium of Thermophysical Property Measurement Methods, Springer, Boston, 1992.
[17] ASTM Standard Test Method for Thermal Conductivity of Solids by Means of the Guarded-Comparative-Longitudinal Heat Flow Technique, ASTM International, West Conshohocken, 2004, pp. E1225–04.
[18] X. Changhu, J. Colby, B. Heng, P. Jeffrey, Uncertainty analysis on the design of thermal conductivity measurement by a guarded cut-bar technique, Meas. Sci. Technol. 22 (2011) 075702. doi:10.1088/0957-0233/22/7/075702
[19] Y. Baek, R. Yonghwan, K. Yong, Structural characterization of β-SiC nanowires synthesized by direct heating method, Mat. Sci. Eng. C 26 (2006) 805–808. doi:10.1016/j.msec.2005.09.083
[20] J. N. Sweet, E. P. Roth, M. Moss, G. M. Haseman, J. A. Anaya, Comparative Thermal Conductivity Measurements at Sandia National Laboratories, Report SAND 86-0840, Sandia National Laboratories, Albuquerque, 1986.
[21] C. G. S. Pillai, A. M. George, An improved comparative thermal conductivity apparatus for measurements at high temperatures, Int. J. Thermophys. 12 (1991) 563–576. doi:10.1007/BF00502369
[22] D. Didion, An Analysis and Design of a Linear Guarded Cut-Bar Apparatus for Thermal Conductivity Measurements, Springfield, National Technical Information Service, 1968.
[23] X. Li, J. J. Yu, Modeling the effects of Cu variations on the precipitated phases and properties of Al-Zn-Mg-Cu alloys, J. Mater. Eng. Perform. 22 (2013) 2970–2981. doi:10.1007/s11665-013-0588-x
[24] C. Hamilton, A. Sommers, S. Dymek, A thermal model of friction stir welding applied to Sc-modified Al-Zn-Mg-Cu alloy extrusions, Int. J. Mach. Tool. Manu. 49 (2009) 230–238. doi:10.1016/j.ijmachtools.2008.11.004
[25] K. V. S. Murthy, D. P. Girisha, R. Keshavamurthy, T. Varol, P. G. Koppad, Mechanical and thermal properties of AA7075/TiO_2/Fly ash hybrid composites obtained by hot forging, Prog. Nat. Sci.-Mater. 27 (2017) 474–481. doi:10.1016/j.pnsc.2017.08.005
[26] Y. S. Touloukian, R. W. Powell, C. Y. Ho, P. G. Klemens, Thermal Conductivity Metallic Elements and Alloys, Volume 1, IFI/Plenum Press, New York, 1970. ISBN 0306670216.
[27] C. Y. Ho, R. W. Powell, P. E. Liley, Thermal conductivity of the elements: A comprehensive review, J. Phys. Chem. Ref. Data 3 (Suppl. 1) (1974) 1–796. doi:10.1063/1.3253100
[28] C. Y. Ho, M. W. Ackerman, K. Y. Wu, S. G. Oh, T. N. Havill, Thermal conductivity of ten selected binary alloy systems, J. Phys. Chem. Ref. Data 7 (1978) 959–1177. doi:10.1063/1.555583
[29] H. Erol, E. Çadirli, E. A. Erol, M. Gündüz, Dependency of the thermal and electrical conductivity on temperatures and compositions of Zn in the Al-Zn alloys, Int. J. Cast Met. Res. 32 (2019) 95–105. doi:10.1080/13640461.2018.1549190
[30] L. Smith, The Development and Processing of Novel Aluminum Powder Metallurgy Alloys for Heat Sink Applications, Master's thesis, Dalhousie University, Halifax, Nova Scotia, 2013.
[31] A. Kalemtaş, G. Topateş, O. Bahadır, P. K. İsçi, H. Mandal, Thermal properties of pressureless melt infiltrated AlN-Si-Al composites, Trans. Nonferrous Met. Soc. China 23 (2013) 1304–1313. doi:10.1016/S1003-6326(13)62598-4
[32] E. J. Sergent, A. Krum, Thermal Management Handbook: For Electronic Assemblies, Mc Graw-Hill, New York, 1998.
[33] E. A. Brandes, Smithells Metals Reference Book, 5th Edition, Butterworth&Co. Ltd. London&Boston, 1976.
[34] J. J. Muhsin, H. T. Moneer, A. M. Muhammed, Effect of friction stir welding parameters (rotation and transverse) speed on the transient temperature distribution in friction stir welding of AA 7020-T53, J. Eng. App. Sci. 7 (2012) 436–446.
[35] G. Wei, P. Huang, C. Xu, D. Liu, X. Ju, X. Du, L. Xing, Y. Yang, Thermophysical property measurements and thermal energy storage capacity analysis of aluminum alloys, Sol. Energy 137 (2016) 66–72. doi:10.1016/j.solener.2016.07.054
[36] E. S. R. Gopal, Specific Heats at Low Temperatures, Plenum Press, New York, 1966.
[37] K. C. Mills, Recommended Values of Thermophysical Properties for Selected Commercial Alloys, National Physical Laboratory and ASM International, Woodhead Publishing Limited, Cambridge, 2002.
[38] C. J. Smithells, General Physical Properties. In: E. A. Brandes, G. B. Brook (Eds.), Metals Reference Book, Butterworth-Heinemann, Oxford, 1992.
[39] Y. S. Touloukian, R. W. Powell, C. Y. Ho, M. C. Nicolaou, Thermophysical Properties of Matter, Volume 10. In: Y. S. Touloukian, C. Y. Ho (Eds.), Thermal Diffusivity, IFI/Plenum, New York, 1973.
[40] S. W. Choi, H. S. Cho, S. Kumai, Effect of the precipitation of secondary phases on the thermal diffusivity and thermal conductivity of Al-4.5Cu alloy, J. Alloys Compd. 688 (2016) 897–902. doi:10.1016/j.jallcom.2016.07.137
[41] Y. M. Kim, S. W. Choi, S. K. Hong, The behavior of thermal diffusivity change according to the heat treatment in Al-Si binary system, J. Alloys Compd. 687 (2016) 54–58. doi:10.1016/j.jallcom.2016.06.080
[42] C. Zhang, Y. Du, S. Liu, S. Liu, W. Jie, B. Sundman, Microstructure and thermal conductivity of the as-cast and annealed Al-Cu-Mg-Si alloys in the temperature range from 25 to 400 °C, Int. J. Thermophys. 36 (2015) 2869–2880. doi:10.1007/s10765-015-1924-1
[43] V. Bykov, S. Uporov, T. Kulikova, Thermal conductivity of Al-Gd-TM glass-forming alloys, Trans. Nonferr. Metal. Soc. China 25 (2015) 1911–1916. doi:10.1016/S1003-6326(15)63798-0